Progress In Electromagnetics Research Letters, Vol. 62, 23–28, 2016

Wideband Bandpass Filter with Multiple Transmission Zeros Using a Shorted Stub-Loaded Stepped-Impedance Ring Resonator

Qian Yang[1, *], Yong-Chang Jiao[1], Zheng Zhang[1], and Nan Wang[2]

Abstract—A wideband bandpass filter with multiple transmission zeros using a shorted stub-loaded stepped-impedance ring resonator is proposed. The resonant characteristics are investigated by even- and odd-mode analysis. In order to obtain a wideband response, the even resonant frequencies can be lowered by the shorted stub and the stepped-impedance ring. The transmission line theory is used to analyze the transmission zeros. Besides the parameters of the shorted stub and stepped-impedance ring, the transmission zeros can also be adjusted by the port separation angle. To verify the proposed design concept, a filter with 132% 3 dB fractional bandwidth and five transmission zeros in the upper stopband is designed, simulated, and fabricated. Good agreement is observed between the simulated and measured results.

1. INTRODUCTION

Wideband bandpass filters (BPFs) with high performance play an important role in microwave communication systems. Modern high data-rate communication systems demand wideband, high-selectivity, and wide stopband filtering property. In addition, the controllable transmission zeros frequencies are very important in transmission signal suppression of the particular frequency response. Various kinds of ultra-wideband (UWB) filters employing short-/open-circuited stubs, parallel-coupled lines, stepped-impedance resonator and multilayer structure [1–8] have been designed and analyzed. The short-/open-circuited stubs [1–5] and stepped-impedance resonator [6, 7] can generate multiple resonant modes to achieve multiple transmission poles in UWB. In order to have good out-of-band performance, the cross coupling short-circuited stubs in [1] introduce a pair of transmission zeros on both sides of the passband, while the stopband width is not wide. A bandstop filter is added to the BPFs in [2, 5, 7] to realize a wide stopband, but the sizes are large. The geometric structure in [10] is designed to shift the third resonance as high as possible, and the transmission zeros created by the structure are also devised to suppress the second resonance to achieve a wide upper stopband. However, the structure is complex. Filters have wide passband [3], good out-of-band performance [4, 11], and compact structure [9] with back-aperture. However, they cannot be integrated easily with other components. Good UWB passband performance is realized by the strong coupling degree of the parallel-coupled line in [6], but the fabrication is difficult. A filter using multilayer liquid crystal polymer technology has compact size [8], while it has complicated structure.

In this paper, a novel shorted stub-loaded stepped-impedance ring resonator is proposed for wideband BPF with good out-of-band performance. The resonant frequencies can be controlled conveniently by the shorted sub and the stepped-impedance ring to obtain a wide passband. Based on transmission line theory, the transmission zeros analyzed by transversal signal concepts are studied as that in [12, 13]. The transmission zeros can also be adjusted easily by the port separation angle to

Received 1 August 2016, Accepted 26 August 2016, Scheduled 1 September 2016

* Corresponding author: Qian Yang (yangqianxidian@126.com).

[1] National Key Laboratory of Antennas and Microwave Technology, Xidian University, Xi'an 710071, P. R. China. [2] State Grid Shaanxi Electric Power Research Institute, Xi'an, Shannxi 710100, P. R. China.

achieve sharp skirts and good suppression in upper band. Finally, a 132% 3 dB fractional bandwidth (FBW) filter with five transmission zeros in upper stopband is designed and fabricated. The measured and simulated results agree well.

2. ANALYSIS OF THE PROPOSED RESONATOR

Figures 1(a) and (b) show the structure and equivalent circuit of the filter discussed in this paper. It consists of a stepped-impedance ring whose characteristic impedances and electrical lengths are Z_a, Z_b, $2\theta_a$, and $2\theta_b$, respectively, and a centrally loaded short-circuited stub with electrical length θ_c and characteristic impedance Z_c is attached at the top of the ring. The characteristic impedances of the two microstrip lines at the input/output ports are all $Z_0 = 50\,\Omega$.

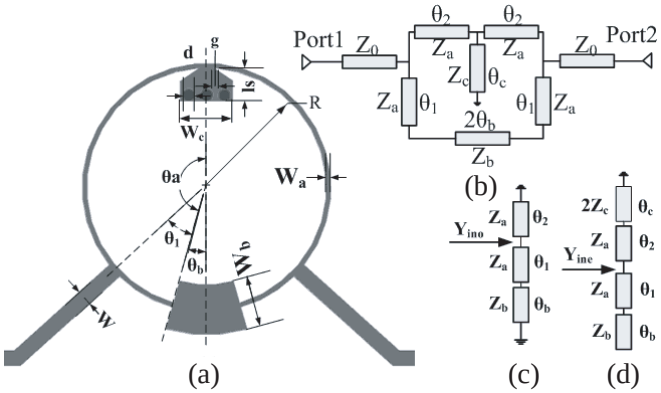

Figure 1. Schematic of the proposed wideband BPF structure. (a) Top view. (b) Equivalent circuit $\theta_1 + \theta_2 = \theta_a$. (c) Equivalent odd-mode circuit. (d) Equivalent even-mode circuit.

The resonant frequencies of the filter can be analyzed using the equivalent even- and odd-mode circuits in Figs. 1(c) and (d). Neglecting the transmission line discontinuity, the odd- and even-mode input admittances can be expressed as follows:

$$Y_{ino} = \frac{1}{jZ_a \tan\theta_2} + \frac{Z_a - Z_b \tan\theta_b \tan\theta_1}{jZ_a(Z_b \tan\theta_b + Z_a \tan\theta_1)} \tag{1}$$

$$Y_{ine} = \frac{Z_a - 2Z_c \tan\theta_c \tan\theta_2}{jZ_a(2Z_c \tan\theta_c + Z_a \tan\theta_2)} + \frac{Z_a + Z_b \cot\theta_b \tan\theta_1}{jZ_a(-Z_b \cot\theta_b + Z_a \tan\theta_1)} \tag{2}$$

The odd- and even-mode resonant conditions can be derived by setting $Y_{ino} = Y_{ine} = 0$ with impedance ratios $R_{zb} = Z_b/Z_a$, $R_{zc} = Z_c/Z_a$. It follows from the resonant conditions that

$$\tan\theta_a + R_{zb} \tan\theta_b = 0 \tag{3}$$

$$R_{zb} \cot\theta_b - 2R_{zc} \tan\theta_c + \tan\theta_a(1 + 2R_{zb}R_{zc} \tan\theta_c \cot\theta_b) = 0 \tag{4}$$

Equation (3) shows that the odd-mode resonant frequency only has relationship with electric lengths θ_a, θ_b and impedance ratio R_{zb}, while (4) indicates the even-mode resonant frequency has relationship with electric lengths θ_a, θ_b, θ_c and impedance ratios R_{zb}, R_{zc}. When the structure of a resonator is chosen, the electric length ratios are fixed. Here we use electric length ratios θ_a/θ_b, θ_c/θ_b to investigate the resonant frequency characteristics. To compare the resonant frequencies of the proposed resonator to that of a simple uniform ring resonator, all resonant frequencies of the proposed resonator are normalized to the first resonant frequency (f_0) of a simple uniform ring resonator at which $\theta_a + \theta_b = \pi$. Also it follows from Eqs. (3) and (4) that the first even-mode resonant frequency is lower than the first odd-mode resonant frequency.

Figure 2(a) plots the normalized odd-mode resonant frequencies versus the electrical length ratio θ_a/θ_b while the impedance ratio R_{zb} has different values. The variation trend of odd-mode resonant frequency with respect to the impedance ratio R_{zb} is the same as that of a stepped-impedance resonator.

It can be concluded from (3) that the changes of the odd-mode resonant frequencies in the case of $R_{zb} < 1$ are opposite to the changes in the case of $R_{zb} > 1$. And the changes of the odd-mode resonant frequencies in the case of $\theta_a/\theta_b < 1$ are opposite to the changes in the case of $\theta_a/\theta_b > 1$. The conclusion can be also observed in Fig. 2(a). The curve of the nth odd-mode resonant frequency has n quasi semi-periods in the range of $0 < \theta_a/\theta_b < 1$. When the electric length ratio θ_a/θ_b is much larger than 1, the odd-mode resonant frequency becomes higher as the impedance ratio R_{zb} becomes smaller. Figs. 2(b), (c), and (d) plot the normalized even-mode resonant frequencies versus the electrical length ratio θ_a/θ_b while one parameter changes and other parameters remain constant. The nth even-mode resonant frequency ratio is smaller than $(2n-1)/2$, and the even-mode resonant frequency curves get flat as θ_a/θ_b flatten. It can be observed that the normalized even-mode resonant frequencies can be lowered by increasing θ_c and R_{zc} or decreasing R_{zb}. Therefore, the first even-mode frequency can be lowered by adjusting the parameters to broaden the passband.

Based on the transmission line theory, the $ABCD$ parameter matrix in Fig. 1(b) can be converted to the Y parameter matrix. The frequencies of transmission zeros can be calculated when the mutual admittance between the two ports equals zero, i.e., $Y_{21} = Y_{12} = 0$ [1]. Thus, we have the following equation

$$\sin 2\theta_1 \cos\theta_b + \sin 2\theta_2 + \sin^2\theta_2 \cot\theta_c/R_{zc} + R_{zb}\sin 2\theta_b \cos^2\theta_1 - \sin 2\theta_b \sin^2\theta_1/R_{zb} = 0 \tag{5}$$

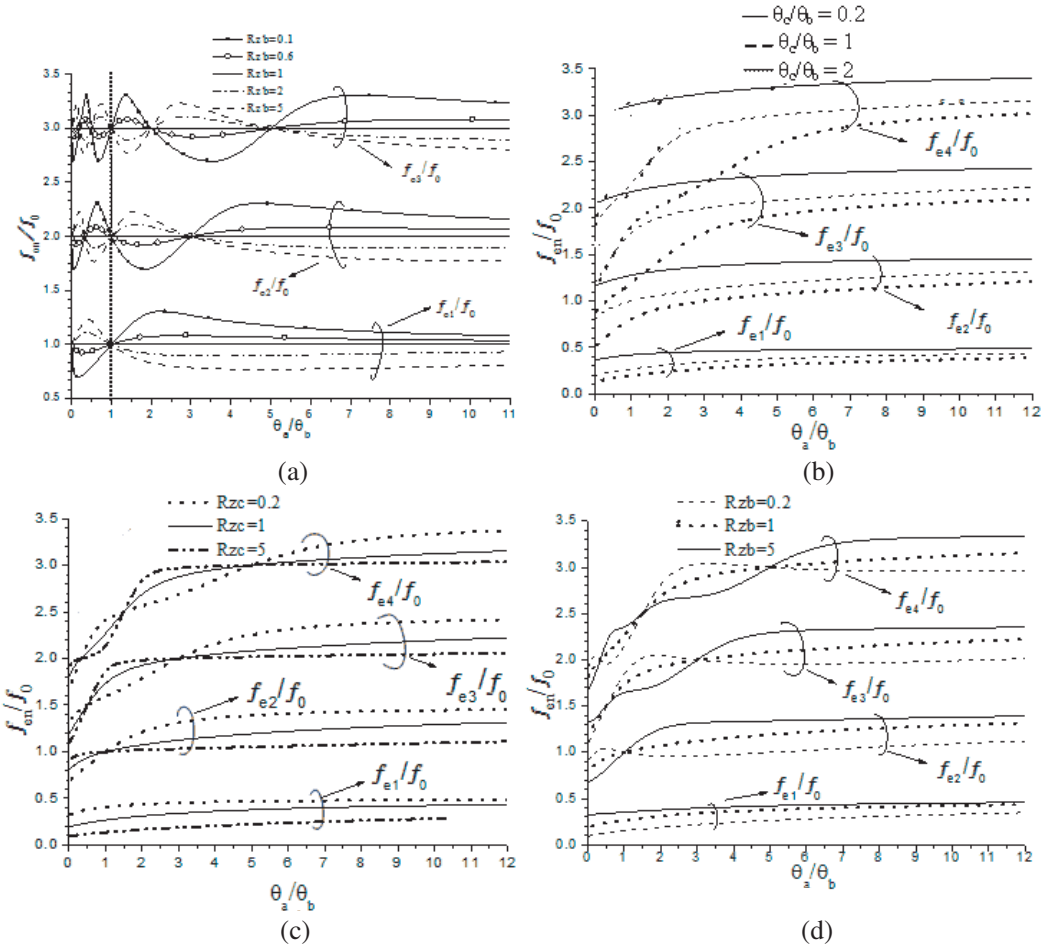

Figure 2. (a) Normalized odd-mode resonant frequencies versus θ_a/θ_b and R_{zb}. (b) Normalized even-mode resonant frequencies versus θ_a/θ_b and θ_c/θ_b when $R_{zb} = R_{zc} = 1$. (c) Normalized even-mode resonant frequencies versus θ_a/θ_b and R_{zc} when $R_{zb} = 1$ and $\theta_c/\theta_b = 1$. (d) Normalized even-mode resonant frequencies versus θ_a/θ_b and R_{zb} when $R_{zc} = 1$ and $\theta_c/\theta_b = 1$.

In order to have sharp skirts and a wide upper stopband, the transmission zeros are designed to be placed at the resonant frequencies in the upper stopband and near the resonant frequency in the passband. So the parameters θ_a/θ_b, θ_c/θ_b, R_{zb} and R_{zc} are firstly chosen to have adjacent even- and odd-mode resonant frequencies. Then the transmission zeros can be adjusted by the port separation angle θ_1, to make them near the resonant frequencies in the upper stopband.

The frequencies of transmission zeros normalized to f_0 versus θ_1/θ_b are plotted in Fig. 3, while other parameters are fixed. The resonant frequencies are also plotted in Fig. 3 to compare with the transmission zeros. It is worth mentioning that the passband performance can be greatly affected by the first and second transmission zero positions. In order to have good in-band and out-of-band performances, we can choose the port separation angle to make the first and second transmission zeros larger than the resonant frequencies in the passband, and other transmission zeros near the resonant frequencies in the upper stopband.

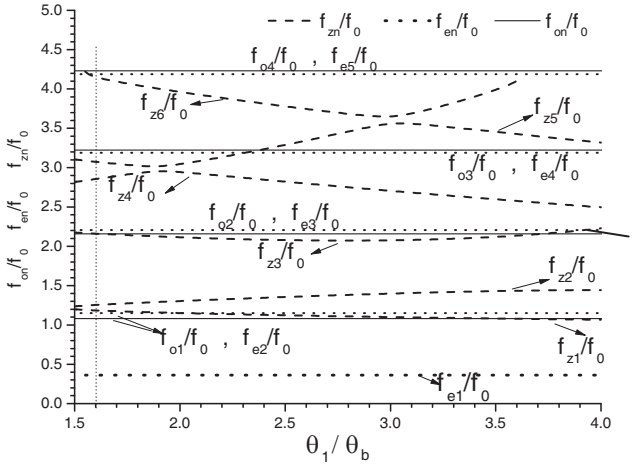

Figure 3. Transmission zero design graph for the resonator with $R_{zb} = 0.2$, $R_{zc} = 0.2$, $\theta_a/\theta_b = 9.5$, and $\theta_c/\theta_b = 0.9$.

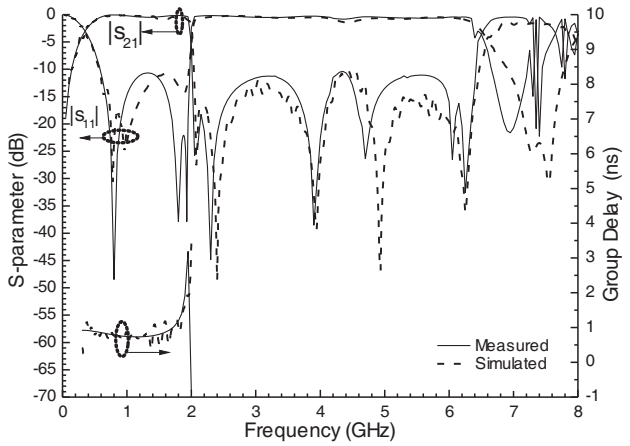

Figure 4. The simulated and measured results for the prototype filter.

3. FILTER DESIGN, FABRICATION AND MEASUREMENT

After the equivalent circuit analysis of the proposed filter, a BPF with passband from 0.35 to 1.95 GHz and five transmission zeros in the upper stopband is designed. Firstly, a ring with circumference equivalent to one waveguide wavelength at frequency 1.55 GHz (f_0) is chosen. To lower the first even-mode resonant frequency (f_{e1}) and have close even- and odd-resonant frequencies, parameters R_{zb}, R_{zc}, θ_a/θ_b and θ_c/θ_b are set to 0.2, 0.2, 9.5 and 0.9, respectively. From Eqs. (3) and (4), there are three resonant modes in the passband, which are two even modes and one odd mode ($f_{e1} = 0.36f_0$, $f_{e2} = 1.15f_0$, and $f_{o1} = 1.08f_0$). The other resonant frequencies are $f_{e3} = 2.2f_0$, $f_{e4} = 3.18f_0$, $f_{e5} = 4.19f_0$, $f_{o2} = 2.16f_0$, $f_{o3} = 3.22f_0$, and $f_{o4} = 4.23f_0$. To have sharp shirts and more transmission zeros in the upper stopband, the electrical length ratio θ_1/θ_b that relates to the port separation angle is set to be 1.6. The frequencies of transmission zeros calculated by Eq. (5) are $f_{z1} = 1.18f_0$, $f_{z2} = 1.26f_0$, $f_{z3} = 2.2f_0$, $f_{z4} = 2.9f_0$, $f_{z5} = 3.1f_0$, and $f_{z6} = 4.2f_0$.

Based on the proposed design method, a BPF is simulated and fabricated on a substrate with $\varepsilon_r = 2.65$, $\tan\delta = 0.003$, and $h = 1$ mm. The dimensions optimized by Ansoft HFSS are $\theta_a = 164°$, $\theta_b = 16°$, $\theta_1 = 32°$, $W = 2.7$ mm, $W_a = 0.8$ mm, $W_b = 8.8$ mm, $W_c = 9.3$ mm, $l_s = 5.5$ mm, $l_c = 3.2$ mm, $R = 21.1$ mm, $g = 1.2$ mm, and $d = 2$ mm. Fig. 4 shows the simulated and measured results for the S-parameters and the group delay. The measured 3 dB FBW is 132%, and the centre frequency is 1.18 GHz (f_c). The measured insertion loss (IL) is found to be less than 0.4 dB at the centre frequency in the passband. The measured 1 dB FBW is 117%. The ILs at some interested frequencies 0.9 (GSM), 1.228 (GPS L2 band), 1.575 (GPS L1 band), and 1.8 GHz (DCS) are 0.32, 0.01, 0.24 and 0.18 dB,

respectively. The retun loss is better than 10 dB. The upper stop bandwidth is from 2 to 6.56 GHz ($5.56f_c$). The measured frequencies of the transmission zeros are 2.07, 2.4, 3.94, 4.93 and 6.26 GHz. The fourth transmission zero is the same as the the fifth transmission zero. The discrepancies between the simulated results and the designed results may be due to the ignoring the effect of the transmission line discontinuity. The filter also has sharp skirts and flat group delay. The measured group delay is less than 1.3 ns within most of the passband. Good agreement is observed between the simulated and measured results. Some minor discrepancies relate to the fabrication tolerances. The photograph of the fabricated filter is shown in Fig. 5. Table 1 shows that the proposed filter in this paper has wider bandwidth, more miniaturized structure, wider stopband, and lower insertion loss simultaneously, than other designs.

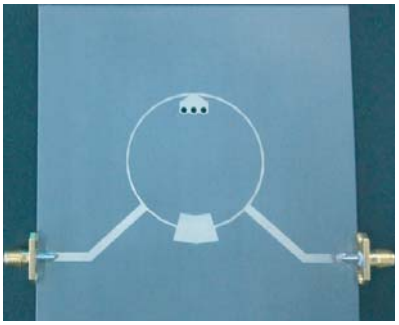

Figure 5. The photograph of fabricated filter.

Table 1. Comparison with the reported wideband BPFs.

Ref.	IL (dB)	3 dB FBW	Upper Stopband (dB)	Effective Size ($\lambda_g \times \lambda_g$)
[1]	0.6	108%	$> 20(1.9f_c)$	0.30×0.41
[2]	< 1.5	110%	$> 30(3.4f_c)$	1.14×0.94
[3]	< 1.5	122%	$> 18(2.6f_c)$	0.51×0.33
[4]	< 2	117%	$> 20(2.4f_c)$	0.514×0.312
[5]	< 1	106%	$> 23.8(2.0f_c)$	0.65×0.25
[6]	0.55	113%	—	0.36×0.05
[7]	0.6	57.9%	$> 18(3.1f_c)$	0.24×0.06
This work	0.4	132%	$> 10(5.56f_c)$	0.18×0.16

λ_g is the guided wavelength at center frequency.

4. CONCLUSIONS

A BPF using a shorted stub-loaded stepped-impedance ring resonator is proposed. Besides tuning the characteristic impedance and electrical length ratios for the shorted stub and the stepped-impedance ring, the port separation angle can also be tuned to adjust the transmission zero positions, resulting in good passband and stopband performance. With a simple structure and good performance, the proposed filter is attractive for wideband BPF applications.

REFERENCES

1. Li, X. P. and X. Ji, "Novel compact UWB bandpass filters design with cross-coupling between $\lambda/4$ short-circuited stubs," *IEEE Microw. Wireless Compon. Lett.*, Vol. 24, No. 1, 23–25, Jan. 2014.

2. Shaman, H. and J. S. Hong, "An optimum ultra-wideband (UWB) band pass filter with spurious response suppression," *Wireless and Microw. Tech. Conf. (WAMICON)*, 1–5, Dec. 2006.
3. Zhu, H. and Q. X. Chu, "Compact ultra-wideband (UWB) bandpass filter using a dual-stub-loaded resonator (DSLR)," *IEEE Microw. Wireless Compon. Lett.*, Vol. 23, No. 10, 527–529, Oct. 2013.
4. Chu, Q. X., X. H. Wu, and X. K. Tian, "Novel UWB bandpass filter using stub-loaded multiple-mode resonator," *IEEE Microw. Wireless Compon. Lett.*, Vol. 21, No. 8, 403–405, Aug. 2011.
5. Tand, C. W. and M. G. Chen, "A microstrip ultra-wideband bandpass filter with cascaded broadband bandpass and bandstop filters," *IEEE Trans. Microw. Theory Tech.*, Vol. 55, No. 11, 2412–2418, Nov. 2007.
6. Zhu, L., S. Sun, and W. Menzel, "Ultra-wideband (UWB) bandpass filters using multiple-mode resonator," *IEEE Microw. Wireless Compon. Lett.*, Vol. 15, No. 11, 796–798, Nov. 2005.
7. Fan, J., D. Z. Zhan, C. J. Jin, and J. R. Luo, "Wideband microstrip bandpass filter based on quadruple mode ring resonator," *IEEE Microw. Wireless Compon. Lett.*, Vol. 22, No. 7, 348–350, Jul. 2012.
8. Qian, S. L. and J. S. Hong, "Miniature quasi-lumped-element wideband bandpass filter at 0.5–2 GHz band using multilayer liquid crystal polymer technology," *IEEE Trans. Microw. Theory Tech.*, Vol. 60, No. 9, 2799–2807, Sep. 2012.
9. Awai, I. and T. Yamashita, "Theory on rotated excitation of a circular dual-mode resonator and filter," *IEEE MTT-S Int. Dig.*, Vol. 2, 781–784, Jun. 1997.
10. Kuo, J.-T., S.-C. Tang, and S.-H. Lin, "Quasi-elliptic function bandpass filter with upper stopband extension and high rejection level using cross-coupled stepped-impedance resonators," *Progress In Electromagnetics Research*, Vol. 114, 395–405, 2011.
11. Gao, M.-J., L.-S. Wu, and J.-F. Mao, "Compact notched ultra-wideband bandpass filter with improved out-of-band performance using quasi electromagnetic bandgap structure," *Progress In Electromagnetics Research*, Vol. 125, 137–150, 2012.
12. Chiou, Y.-C., P.-S. Yang, J.-T. Kuo, and C.-Y. Wu, "Transmission zero design graph for dual-mode dual-band filter with periodic stepped-impedance ring resonator," *Progress In Electromagnetics Research*, Vol. 108, 23–36, 2010.
13. Xue, S., W. Feng, H. Zhu, and W. Che, "Microstrip wideband bandpass filter with six transmission zeros using transversal signal-interaction concepts," *Progress In Electromagnetics Research C*, Vol. 34, 1–12, 2013.